

## Formation of Nanosized Organic Molecular Crystals on Engineered Surfaces

Kitae Kim,<sup>†</sup> In sung Lee,<sup>†</sup> Andrea Centrone,<sup>‡</sup> T. Alan Hatton,<sup>‡</sup> and Allan S. Myerson<sup>\*†</sup>

*Department of Chemical and Biological Engineering, Illinois Institute of Technology, Chicago, Illinois 60616, and  
Department of Chemical Engineering, Massachusetts Institute of Technology, 77 Massachusetts Avenue,  
Cambridge, Massachusetts 02139*

Received September 22, 2009; E-mail: myerson@iit.edu

The formation of organic molecular crystals with sizes below 500 nm is of great interest to the pharmaceutical industry since an enhanced solubility and dissolution rate can potentially increase drug bioavailability. In this work, patterned engineered surfaces were used for crystallizing glycine with a lateral dimension below 200 nm in a confined volume while controlling supersaturation. Individual crystals were characterized with AFM and Raman spectroscopy and determined to be the metastable  $\beta$  form. The solubility of crystals obtained was measured as a function of crystal size and employed along with the Ostwald–Freundlich equation to predict solubility enhancement vs crystal size.

Methods to produce nanosized organic molecular crystals include both ‘top down’ and ‘bottom up’ approaches.<sup>1,2</sup> Top down methods, such as milling and high pressure homogenization, employ crystal or particle breakage and can impact the stability and crystallinity of the solid. Bottom up methods, such as supercritical fluid crystallization and impinging jet crystallization, exploit high levels of supersaturation and can lead to the formation of amorphous materials and/or oils or an undesired crystalline form (polymorph). These issues have generated interest in methods for producing nanosized organic molecular crystals at low supersaturations. Recent work has focused on methods that confine the crystallization volume, such as emulsions<sup>3</sup> and nanoporous materials.<sup>4</sup> The method described in this work controls both supersaturation and crystallization volume while providing a template for nucleation.

In previous studies, patterned Self Assembled Monolayers (SAMs) were used to produce micrometer sized crystals of organic compounds.<sup>5</sup> Hydrophilic islands surrounded by hydrophobic regions were used to form arrays of small hemispherical droplets when wetted with polar solutions. The size of the hydrophilic islands influenced the final crystal size because crystallization was constrained in each hemispherical droplet. In addition, the concomitant nucleation of polymorphs was demonstrated in a number of systems.<sup>5</sup> Here, we fabricated bifunctional (hydrophilic and hydrophobic) patterned surfaces with circular shaped islands with diameters of 500 nm using photolithography and SAMs as shown in Figure 1a (see Supporting Information (SI) for details). The circular islands were covered with a hydrophilic SAM (3-amino-propyl-triethoxysilane (ATPES)), while the rest of the surface was functionalized with a hydrophobic SAM (octadecyltrichlorosilane (OTS)). The diameter of the solution droplets generated on each hydrophilic island was below 500 nm, and consequently, the crystal size formed on each island could be controlled to be smaller than 500 nm.

Glycine, the simplest amino acid, was selected as the model compound for this study, because the nucleation and polymorphism of glycine has been studied in depth.<sup>5,6</sup> Figure 1b illustrates our

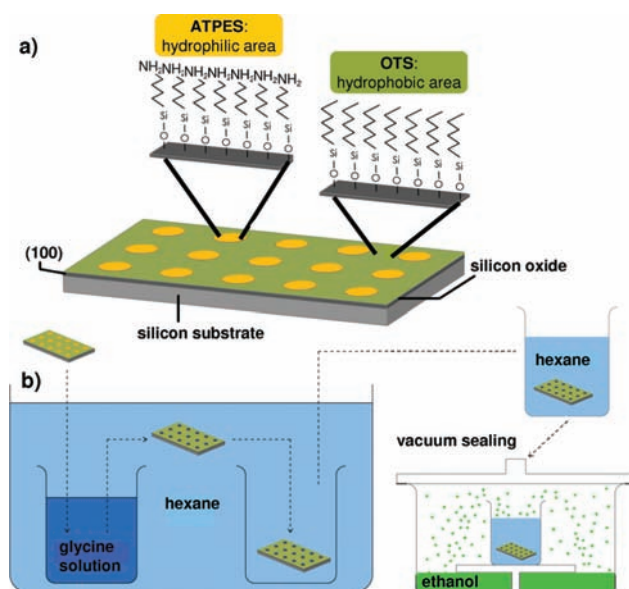


**Figure 1.** (a) Schematic representation of the bifunctional SAMs pattern. (b) Schematic representation of the glycine crystallization procedure; the supersaturation level is controlled by the slow diffusion of an antisolvent (ethanol) into the glycine/water solution.

approach for controlling supersaturation to obtain nanosized crystals on the bifunctional substrate. A glass jar containing an aqueous undersaturated glycine solution was immersed into a vessel filled with hexane. Since hexane is immiscible with water<sup>7</sup> and the solubility of glycine in hexane is extremely low, the two solutions remained separated. The aqueous glycine solution has a higher density than hexane and was placed at the bottom of the vessel. The patterned substrate was immersed into the glycine solution and slowly retracted into hexane without exposing it to air. The glycine solution wetted the hydrophilic circular islands, generating arrays of 500 nm hemispherical solution droplets on the substrate surface covered by hexane. The array of glycine solution droplets remained undersaturated since the hexane prevented evaporation. The supersaturation level of the glycine droplets was controlled by allowing diffusion of an antisolvent (ethanol) into the droplets. The glass jar with hexane protecting the substrate was placed into a desiccator with ethanol on the bottom and then sealed with vacuum grease. Supersaturation was generated slowly by ethanol diffusion first into the hexane then into the aqueous glycine droplets. As the ethanol diffused into the droplets, the solubility of glycine was reduced,<sup>8</sup> and after 70 h glycine crystals were formed.

By controlling the initial glycine concentration and the rate of diffusion (and thus the supersaturation profile), we were able to produce glycine crystals ranging in size from  $180 \times 160 \times 57 \text{ nm}^3$  ( $2.59 \times 10^{-12} \text{ mg}$ ) to  $250 \times 220 \times 74 \text{ nm}^3$  ( $6.42 \times 10^{-12} \text{ mg}$ ). Figure 2 shows

<sup>†</sup> Illinois Institute of Technology.

<sup>‡</sup> Massachusetts Institute of Technology.

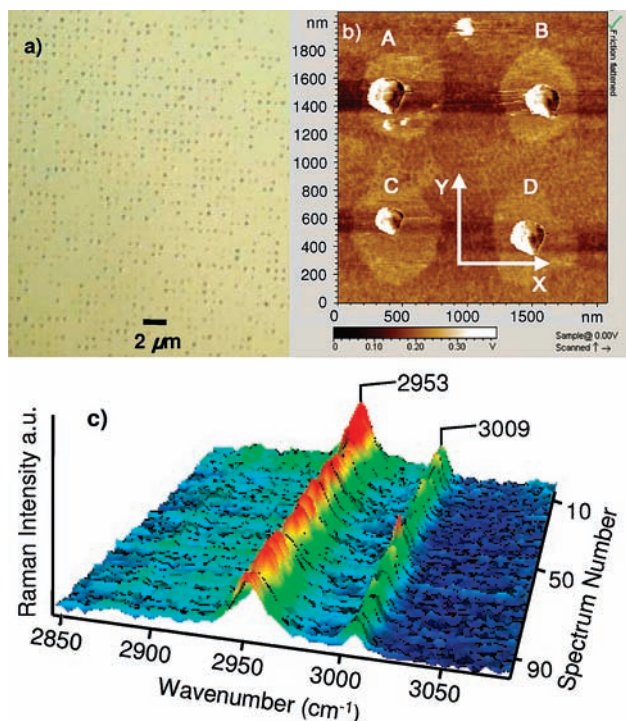


**Figure 2.** (a) Optical microscope image ( $\times 150$ ) of  $1600 \mu\text{m}^2$  and (b) AFM image of  $4 \mu\text{m}^2$  of the  $500 \text{ nm}$  patterned SAMs on the silicon substrate. The crystals dimensions are: (A)  $250 \times 220 \times 74 \text{ nm}^3$ , (B)  $230 \times 205 \times 70 \text{ nm}^3$ , (C)  $180 \times 160 \times 57 \text{ nm}^3$ , and (D)  $220 \times 190 \times 65 \text{ nm}^3$ . (c) Raman spectra of 100 individual glycine crystals found on the patterned SAMs. All crystals were determined to be  $\beta$  form.

the microscope and AFM images of the glycine crystals on the substrate. The microscope image on the left ( $40 \mu\text{m} \times 40 \mu\text{m}$ ) shows that 1600 individual crystals could be placed in this area, while the image on the right ( $2 \mu\text{m} \times 2 \mu\text{m}$ ) depicts four crystals (see also SI). The Raman spectra of 100 individual crystals randomly selected on the substrate were collected using Confocal Raman Microscopy (Figure 2 and SI). All the Raman spectra of the analyzed crystals exhibited the characteristic peaks of the metastable  $\beta$  form.<sup>5</sup> As the  $\beta$  form of glycine is normally obtained from alcohol–water mixtures, this is consistent with the previous studies of glycine polymorphism.<sup>9</sup> Crystals with lateral dimensions below  $100 \text{ nm}$  and heights below  $10 \text{ nm}$  were produced and observed using AFM; however, the solid form could not be characterized (see SI).

One of the assumed advantages of nanosized crystals below  $500 \text{ nm}$  is increased solubility; however data on the solubility enhancement of such organic molecular crystals generally have not been measured.<sup>10</sup> In this work, the methanol solubility of nanosized glycine crystals was measured by observing whether these crystals dissolved in supersaturated glycine solutions of different concentrations (see SI for details). The crystals attached to the substrate were placed in  $100 \text{ mL}$  of supersaturated solutions with concentrations ranging from  $0.328 \text{ mg/mL}$  to  $0.382 \text{ mg/mL}$  (the equilibrium solubility of  $\beta$  glycine in methanol is  $0.290 \pm 0.01 \text{ mg/mL}$ ). The solutions were removed and the surfaces were examined to determine if the crystals had dissolved. The results showed that the solubility increased by  $31.7\%$  for the  $244 \text{ nm}$  crystals,  $22.1\%$  for the  $348 \text{ nm}$  crystals,  $13.1\%$  for the  $598 \text{ nm}$  crystals, and  $8.6\%$  for the  $869 \text{ nm}$  crystals. With these experimental results, the interfacial tension could be calculated using the Ostwald–Freundlich equation.<sup>11</sup> The average value obtained was  $1929 \pm 85 \text{ erg/cm}^2$ . The solubility of crystals as a function of size was then calculated

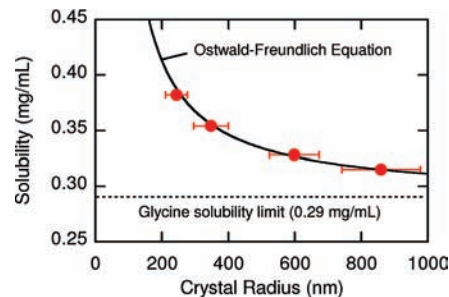


**Figure 3.** Methanol solubility of  $\beta$  glycine crystals as a function of crystal size; experimental data (red dots) and calculated values from the Ostwald–Freundlich equation.

using the Ostwald–Freundlich equation with results as shown in Figure 3. From this calculation the estimated solubility of  $100 \text{ nm}$  sized (radius) crystals is  $0.589 \text{ mg/mL}$  which is approximately twice the equilibrium solubility ( $0.290 \text{ mg/mL}$ ).

In this work crystallization in a constrained environment was used to prepare organic molecular nanocrystals. The control of supersaturation during nucleation and crystal growth should allow control of the crystal form (polymorph). While this work employed organic vapor diffusion to obtain the metastable beta form of glycine, other methods of supersaturation generation such as slow cooling and slow evaporation are currently being evaluated as a means of preparing the alpha and gamma forms of glycine. The methods described here are also being used to prepare nanosized pharmaceutical crystals to aid the formulation of poorly soluble drugs. A major challenge in employing our method is the removal of crystals from the surface. While physical methods such as scraping and ultrasonics are possible, more elegant and efficient methods such as the use of SAMs whose functional group or backbone degrades with temperature and/or with light are being evaluated.

**Acknowledgment.** Financial support by the Office of Naval Research (N00173-06-1-G007) is gratefully acknowledged.

**Supporting Information Available:** Details on the sample preparation, characterization methods, and AFM images of smaller crystals. This material is available free of charge via the Internet at <http://pubs.acs.org>.

## References

- (1) Keck, C. M.; Peters, K. *Eur. J. Pharm. Biopharm.* **2006**, *62*, 3.
- (2) Rainbow, B. E. *Nat. Rev. Drug Discovery* **2004**, *3*, 785.
- (3) Utiye-Ishii, K.; Kwon, E.; Kasai, H.; Nakanishi, H.; Oikawa, H. *Cryst. Growth Des.* **2008**, *8*, 369.
- (4) Hamilton, B. D.; Hillmyer, M. A.; Ward, M. D. *Cryst. Growth Des.* **2008**, *8*, 3368.
- (5) (a) Lee, A. Y.; Lee, I. S.; Dette, S. S.; Boerner, J.; Myerson, A. S. *J. Am. Chem. Soc.* **2005**, *127*, 14982. (b) Lee, I. S.; Lee, A. Y.; Myerson, A. S. *Pharm. Res.* **2008**, *25*, 960. (c) Lee, I. S.; Kim, K. T.; Lee, A. Y.; Myerson, A. S. *Cryst. Growth Des.* **2008**, *8*, 108. (d) Singh, A.; Lee, I. S.; Myerson, A. S. *Cryst. Growth Des.* **2009**, *9*, 1182.
- (6) (a) Garetz, B. A.; Matic, J.; Myerson, A. S. *Phys. Rev. Lett.* **2002**, *89*, 175501. (b) Ferrari, E. S.; Davey, R. J.; Cross, W. I.; Gillon, A. L.; Towler, C. S. *Cryst. Growth Des.* **2003**, *3*, 53. (c) Towler, C. S.; Davey, R.; Lancaster, R. W.; Price, C. J. *J. Am. Chem. Soc.* **2004**, *126*, 13347. (d) Weissbuch, I.; Zbaida, D.; Addadi, L.; Leiserowitz, L.; Lahav, M. *J. Am. Chem. Soc.* **1987**, *109*, 1869.
- (7) Lide, D. R. *CRC Handbook of Chemistry and Physics*; CRC Press LLC: Boca Raton, London, New York, Washington, D.C., 2002.
- (8) Ferreira, L. A.; Macedo, E. A.; Pinho, S. P. *Chem. Eng. Sci.* **2004**, *59*, 31174.
- (9) Weissbuch, I.; Torbeev, V. Yu.; Leiserowitz, L.; Lahav, M. *Angew. Chem., Int. Ed.* **2005**, *44*, 3226.
- (10) (a) Hammond, R. B.; Pencheva, K.; Robert, K. J.; Auffret, T. *J. Pharm. Sci.* **2007**, *96*, 1967. (b) Jinno, J.; Kamada, N.; Miyake, M.; Yamada, K.; Mukai, T.; Odomi, M.; Toguchi, H.; Liversidge, G. G.; Higaki, K.; Kimura, T. *J. Controlled Release* **2006**, *111*, 56.
- (11) Mullin, J. W. *Crystallization*; Butterworth-Heinemann: Oxford, U.K., 2001.

JA908055Y